

Antiferromagnetic ordering in a 90 K copper oxide superconductor

J. A. Hodges,¹ Y. Sidis,² P. Bourges,² I. Mirebeau,² M. Hennion,² and X. Chaud³

¹DRECAM-SPEC, CE-Saclay, 91191 Gif sur Yvette, France

²Laboratoire Léon Brillouin, CEA-CNRS, CE-Saclay, 91191 Gif sur Yvette, France

³CRETA, CNRS, 25 Avenue des Martyrs, BP 166, 38042 Grenoble cedex, France

(Received 5 April 2002; published 24 June 2002)

Using elastic neutron scattering, we evidence a commensurate antiferromagnetic Cu(2) order (AF) ($T_N \sim 330$ K, $\mu \sim 0.14 \mu_B$) in the superconducting (SC) high- T_c cuprate $\text{YBa}_2(\text{Cu}_{1-y}\text{Co}_y)_3\text{O}_{7+\delta}$ ($y=0.013, T_c=93$ K). We find that the spin excitation spectrum is still dominated by a magnetic resonance peak at 41 meV as in the Co-free system, but with a reduced spectral weight. The substitution of Co leads to a state where AF and SC cohabit at a microscopic scale, without any strong interference.

DOI: 10.1103/PhysRevB.66.020501

PACS number(s): 74.72.Bk, 75.40.Gb, 78.70.Nx

The existence of an interplay between magnetic order and superconductivity appears to be a ubiquitous phenomenon in strongly correlated systems, such as high- T_c cuprates,¹⁻⁵ low- T_c ruthenates,⁶ and heavy fermions.^{7,8} In well underdoped $\text{YBa}_2\text{Cu}_3\text{O}_{6+x}$ ($x=0.5-0.6$) for example, elastic neutron scattering (ENS) studies provide evidence for the simultaneous presence of d -wave superconductivity and of Cu(2) magnetic order.^{4,5} However, in the cuprates, it remains a matter of discussion whether magnetic order and superconductivity really coexist or whether there is a microscopic phase segregation. Especially, the role played by disorder is still an open question.^{9,10} In this report, we evidence the appearance of an antiferromagnetic (AF) order in the CuO_2 planes of a fully oxygenated superconducting $\text{YBa}_2\text{Cu}_3\text{O}_7$ based system with $T_c=93$ K, when disorder is introduced by substituting cobalt atoms at the copper site of the chains.

The $\text{YBa}_2\text{Cu}_3\text{O}_{6+x}$ perovskite structure contains two copper sites: Cu(1) belonging to the Cu-O chains (along the b axis), and Cu(2) belonging to the CuO_2 planes. Co^{3+} ions substitute only at the Cu(1) sites.¹¹ Since the Co has a higher oxidation state than the Cu(1), the Co pulls in extra oxygen to increase its oxygen coordination. Each added Co atom, with an average coordination number of 5, pulls in 0.5 oxygen atoms.¹¹⁻¹⁴ In addition, the substitution of Co induces a transverse distortion of its Cu(1) site.^{13,14} Co atoms tend to form either small clusters like dimers^{11,14} or even short chains along the (110) direction.¹³ These chains pin down the twin boundaries of the orthorhombic structure (microtwinning) and trigger the change to the tetragonal phase that occurs near $y=0.025$.¹⁵ Nuclear magnetic resonance (NMR) (Ref. 16) and transport measurements¹⁷ show the cobalt substitution reduces the hole doping. However, for the low Co substitution level ($y \approx 0.013$) examined here, despite the decrease in the Hall effect derived carrier density¹⁷ and in the specific heat derived condensate density,¹⁸ the doping is still high enough for T_c to remain at its optimum value. In addition, nuclear quadrupole resonance (NQR) (Ref. 19) measurements have evidenced the appearance of magnetic moments at the Cu(1) sites and more surprisingly at the Cu(2) sites as well. Mössbauer probe measurements²⁰ have also evidenced the moments at the Cu(2) sites.

We present a neutron scattering study of the magnetic properties of a large single crystal (1.4 cm^3) of fully oxy-

genated $\text{YBa}_2(\text{Cu}_{1-y}\text{Co}_y)_3\text{O}_{7+\delta}$. The sample was prepared by the top-seed melt texturing method. A microprobe analysis confirmed the Co content was that of the starting mixture, $y=0.013$ and showed the Co was uniformly distributed on the μm scale. Neutron depolarization measurements [Fig. 4(c)] provided $T_c=93$ K.

The neutron scattering experiments were made with the triple axis spectrometers 1T1 and 4F2 at the Laboratoire Léon Brillouin, Saclay (France). For the elastic measurements (ENS) on 4F2, a PG(002) monochromator and analyzer were used and a beryllium filter was inserted into the scattered beam in order to remove higher order contamination. The data were taken with a fixed final wave vector of 1.55 \AA^{-1} . For the inelastic measurements (INS) on 1T1, a focusing Cu(110) monochromator and a PG(002) analyzer were used and a pyrolytic graphite filter was inserted into the scattered beam. The data were taken with a fixed final wave vector of 4.1 \AA^{-1} . Measurements were carried out with the crystal in two different orientations where wave vector transfers of the form $\mathbf{Q}=(H,H,L)$ and $(3H,H,L)$ were respectively accessible. Throughout this article, the wave vector \mathbf{Q} is indexed in units of the reciprocal tetragonal lattice vectors $2\pi/a=2\pi/b=1.63 \text{ \AA}^{-1}$ and $2\pi/c=0.53 \text{ \AA}^{-1}$. In this notation the $(\pi/a, \pi/a)$ wave vector parallel to the CuO_2 planes corresponds to points of the form $(h/2, k/2)$ with h and k odd integers.

We first describe the observation of the commensurate magnetic order. Figure 1 shows the elastic neutron intensity at the AF wave vector $\mathbf{Q}=(0.5,0.5,1)$ along both the (110) and (001) directions. The peak, absent at 338 K and present at 250 and 40 K, evidences the magnetic order. Different AF peaks, $\mathbf{Q}=(0.5,0.5,L)$ with L integer, are reported in Fig. 1(c) where magnetic intensity is sizeable at $L=1,2,3$. The observed pattern [Fig. 1(c)] and the absence of any magnetic peak at $\mathbf{Q}=(0.5,0.5,0)$ implies that the magnetic response is fully dominated by magnetic moments at the Cu(2) sites. Gaussian fits of Fig. 1 at different temperatures shows that the AF order is resolution limited, meaning that the correlation lengths are typically $\xi > 200 \text{ \AA}$.

The temperature dependence of the neutron scattering intensity measured at the AF wave vector $\mathbf{Q}=(0.5,0.5,1)$ [Fig. 1(d)] shows the system orders at $T_N \sim 330$ K. As the tem-

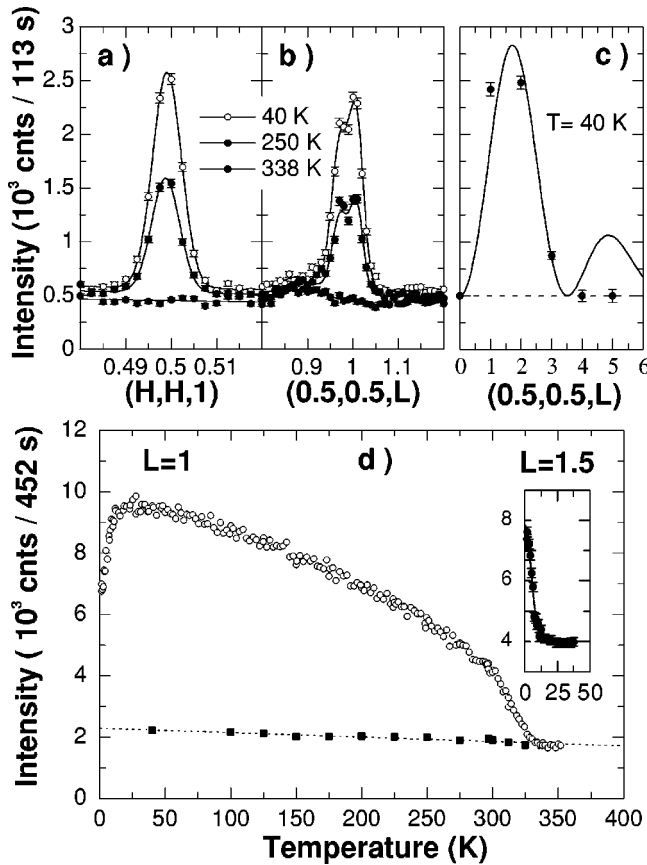


FIG. 1. Elastic neutron intensity along (a) the (110) direction and (b) the (001) direction around $\mathbf{Q}=(0.5,0.5,1)$. (c) L dependence of magnetic intensity at different AF peaks, $\mathbf{Q}=(0.5,0.5,L)$. The full line represents the magnetic intensity expected from in-plane Cu(2) spins with an isotropic Cu²⁺ form factor and including the resolution correction. (d) Temperature dependences of the neutron scattering intensity at $\mathbf{Q}=(0.5,0.5,1)$. The full squares represent the background from scans as shown in (a) and (b). Inset of (d) shows the appearance of magnetic intensity at $\mathbf{Q}=(0.5,0.5,1.5)$ below $T_m=12$ K where the peak at $\mathbf{Q}=(0.5,0.5,1)$ displays a re-entrant behavior.

perature is lowered, the AF Bragg intensity initially increases continuously and no anomaly is observed on passing through T_c . The peak intensity displays a marked downturn at $T_m \approx 12$ K, and almost half of its intensity is left as $T \rightarrow 0$. Below T_m , additional neutron intensity occurs at $L=1.5$ indicating the system undergoes an AF-I-AF-II transition, characterized by the doubling of the AF unit cell along the c axis. This transition is also observed in $\text{YBa}_2\text{Cu}_3\text{O}_6$ when substituted at the Cu(1) site^{21,22} and AFII ordering is observed in nonsuperconducting $\text{YBa}_2(\text{Cu}_{1-y}\text{Co}_y)_3\text{O}_{7+\delta}$ with high Co substitution levels.²³ In the present case, the observed change in ordering may be linked to the influence of magnetic freezing which is known to exist in similar samples. For example, in $\text{YBa}_2(\text{Cu}_{0.94}\text{Co}_{0.06})_3\text{O}_{7+\delta}$, time of flight neutron scattering measurements²⁴ have evidenced the progressive freezing of the Co moments as the temperature is lowered. Freezing has also been evidenced in Co substituted samples by local probe measurements.^{19,20}

The rocking scan around the nuclear Bragg reflection

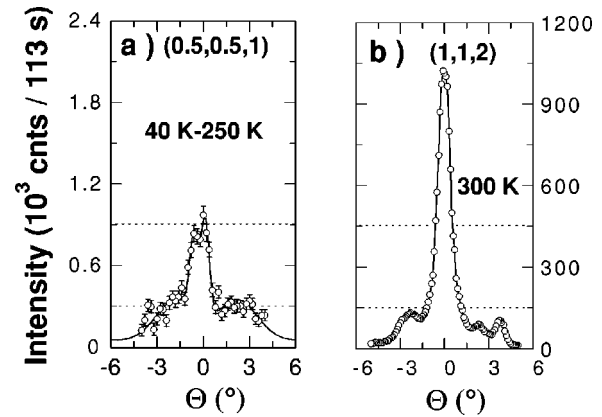


FIG. 2. (a) Difference between the rocking scans at $T=40$ and 250 K around the AF Bragg reflection (0.5,0.5,1). (b) Rocking scan at 300 K around the nuclear Bragg reflection (1,1,2).

(1,1,2) [Fig. 2(b)] shows some structure and indicates the sample is made up of a main part with a mosaic [full width at half maximum (FWHM)] of $\sim 1^\circ$ and some subsidiary parts extending to $\sim 4^\circ$. The difference between rocking scans at 40 and 250 K around the AF Bragg reflection (0.5,0.5,1) [Fig. 2(a)] shows an analogous structure. The magnetic mosaic does not, however, strictly reproduce the nuclear mosaic: the main peak splits into two narrow peaks and the relative scattering intensity of the main part is reduced relative to the subsidiary part. This indicates that the volume of the AF region is reduced compared to the volume of the sample. The fraction of Cu(2) sites carrying an ordered magnetic moment (\mathcal{R}) is thus less than 1. The AF Bragg intensity is proportional to the square of the staggered moment (μ) times \mathcal{R} . With the value $\mathcal{R}=0.5$ (see below), the measured intensity at $T=40$ K corresponds to $\mu=0.14 \pm 0.07 \mu_B$.

We next present the inelastic magnetic fluctuations around the AF wave vector. In cobalt-free optimally doped $\text{YBa}_2\text{Cu}_3\text{O}_{7-\delta}$, the AF correlations are purely dynamic, and the spin excitation spectrum in the superconducting state is characterized by a sharp antiferromagnetic excitation peaked at 41 meV, the so-called “magnetic resonance peak”^{25,26}. In our cobalt substituted sample, we looked for this magnetic excitation which is a signature of d -wave superconductivity and we carried out constant energy scans at 39 meV around $\mathbf{Q}=(0.5,0.5,-5.4)$ along the (110) direction as well as around (1.5,0.5,-1.7) along the (310) direction (Fig. 3). A peak, centered at the AF wave vector, shows up at low temperature in each of the scans. The variation of the ratio of the intensity of the scans as a function of \mathbf{Q} is similar to that of the Cu²⁺ anisotropic magnetic form factor.²² In each scan, the peak diminishes drastically at T_c . Some weak intensity, peaked at the AF wave vector, remains above T_c , as it does in the Co-free compound $\text{YBa}_2\text{Cu}_3\text{O}_{6.97}$.²⁶ After subtracting the scan just above T_c from that at low temperature, the remaining intensity was fitted to a Gaussian profile centered at the AF wave vector. For both types of constant energy scan in Fig. 3, the AF response at 39 meV in the superconducting state has a momentum width (FWHM) of $0.28 \pm 0.06 \text{ \AA}^{-1}$. This momentum distribution is similar to that of the magnetic resonance peak in the Co-free system.²⁶

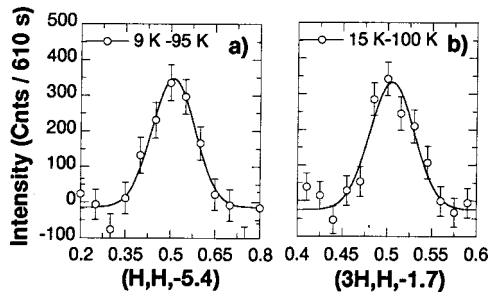


FIG. 3. Difference of constant energy scans performed at 39 meV measured at low temperature and just above T_c : (a) around $Q=(0.5,0.5,-5.4)$ along the (110) direction; (b) around $Q=(1.5,0.5,-1.7)$ along the (310) direction. Solid lines are fits with a Gaussian line shape.

Figure 4 shows energy scans performed at $Q=(0.5,0.5,-5.4)$ both at low temperature and just above T_c . The enhancement of the AF response around 41 meV (the magnetic resonance peak) is visible in the raw data and it is further confirmed by the differences shown on Fig. 4(b). The magnetic resonance peak is not sharp in energy and can be fitted by the usual “ansatz” of a single Gaussian line shape: this yields an intrinsic energy width of $\sim 9 \pm 1$ meV (FWHM). A similar energy broadening of the magnetic resonance peak is reported for Ni and Zn substitutions [at the Cu(2) site] in $\text{YBa}_2\text{Cu}_3\text{O}_{7-\delta}$,²⁸ and in $\text{Bi}_2\text{Sr}_2\text{CaCu}_2\text{O}_{8+\delta}$:²⁹ this indicates the extreme sensitivity of the resonance peak energy width to disorder. The analysis in terms of a single broad signal centered at E_r is supported by the temperature dependences at the AF wave vector at 42 and 35 meV (6 meV below E_r) both of which show a similar decrease of the AF response up to T_c [Fig. 4(c)]. As a function of temperature, the magnetic resonance peak disappears at T_c without any significant shift of its characteristic energy [Fig. 4(b)]. Furthermore, its energy and momentum integrated intensity, calibrated in absolute units against the phonon at 42.5 meV, is $\sim 0.025 \mu_B^2$, that is, it is about half that reported in the Co-free compound.²⁷

Summarizing, the substitution of magnetic Co^{3+} at the chain sites thus introduces a very specific perturbation which induces a commensurate AF three-dimensional (3D) order, below $T_N \sim 330$ K, at the copper sites of the CuO_2 planes, without producing any reduction in T_c . The 41 meV resonance peak is still present, but with a reduced spectral weight. A key question is how does the superconductivity and the antiferromagnetic order cohabit?

To address this issue, we first consider the possibility of complete phase segregation, such that only a small fraction of Cu(2) atoms, for example those adjacent to a Co atom, carries the full magnetic moment of the undoped cuprates ($0.6 \mu_B$). The concentration of Cu(2) moments (in the planes) needed to account for the observed scattering intensity would then be $\mathcal{R} \sim 0.03$, a value which is roughly comparable to the Co substitution level (in the chains). Since the magnetic correlation length exceeds 200 \AA , the Co would be essentially concentrated within these clusters. The local Co concentration would then be quite high and we would expect to observe the behavior seen in bulk samples having

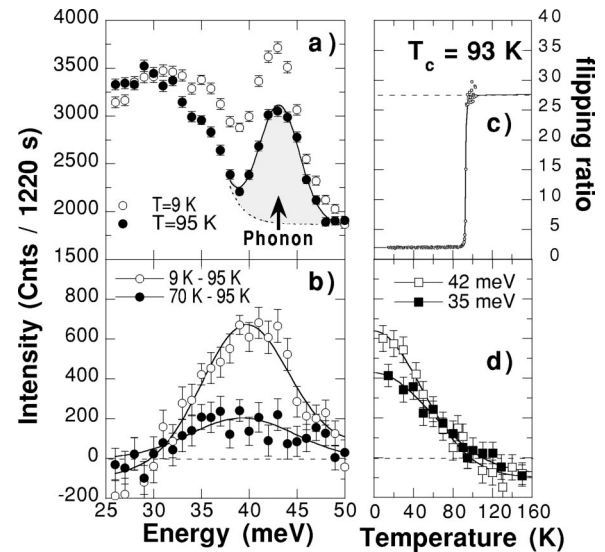


FIG. 4. (a) Energy scans performed at $Q=(0.5,0.5,-5.4)$ at $T=9.2$ and 95 K. The scan above T_c looks very similar to that in the Co-free sample with the phonon peak at 42.5 meV (Ref. 26). (b) Difference between energy scans performed at 9.2 K (or 70 K) and at 95 K. (c) Determination of $T_c=93$ K by the neutron depolarization technique. (d) Temperature dependence of the AF response at 35 and 42 meV.

high Co levels. However, insulating samples of $\text{YBa}_2(\text{Cu}_{1-y}(\text{Co},\text{Fe})_y)_3\text{O}_{7+\delta}$ show the AFII structure up to $T_N \sim 400$ K,^{21,23} whereas it is the AFI structure that is observed here at T_N . A complete phase segregation associated with large local concentrations of Co can thus be ruled out. Further, in $\text{YBa}_2(\text{Cu}_{1-y}\text{Co}_y)_3\text{O}_{7+\delta}$, local probe Cu-NQR (Ref. 19) and Y -NMR (Ref. 16) measurements evidence features that are different from those of the undoped insulating AF state. There are thus strong arguments against the existence of charge segregation into separate hole rich and hole poor regions having different magnetic properties.

Following the reduction of the volume of the AF region compared to the volume of the sample (Fig. 2) and the observed 50% reduction in the weight of the resonance peak: it is possible that distinct SC regions occupy about half of the sample volume leaving the remainder for the distinct magnetically ordered regions ($\mathcal{R} \approx 0.5$, $\mu \approx 0.14 \mu_B$). This viewpoint is consistent with the local probe Cu NQR (Ref. 19) and Mössbauer²⁰ measurements on samples with the same low Co substitution level as here, which show that over 50% of the Cu(2) carry magnetic moments. Our analysis therefore suggests that there is no evidence of any significant variation in the hole doping level but that there are two different local order parameters (superconductivity and magnetic order). Recent scanning tunneling microscope (STM) studies of the underdoped $\text{Bi}_2\text{Sr}_2\text{CaCu}_2\text{O}_{8+\delta}$ have also revealed an apparent segregation of the electronic structure into SC domains of nanoscale size located in an electronically distinct background.³⁰

According to our microprobe analysis, Co impurities are uniformly distributed on a μm scale. At a more microscopic scale, Co atoms aggregate into dimers or small clusters forming lines along the (110) direction.¹³ We speculate that these

lines of magnetic Co atoms are the perturbing elements which induce the AF order into the CuO_2 planes and fashion the observed AF structure. We recall, however, that the Cu(2) moments are not confined to the immediate vicinity of these lines for the magnetic correlation lengths greatly exceed the lateral dimensions of a twin boundary. The AF order in the present case could have its origin in the magnetic polarization produced by the Co^{3+} or in the structural effects related to the microtwinning along the (110) directions¹⁵ or more probably, to a combination of both these effects.

The substitution of Nd for La in $\text{La}_{2-x}\text{Sr}_x\text{CuO}_4$ leads to a state where SC and incommensurate AF (stripe) orders cohabit and with a spin-spin correlation length $\xi \sim 200 \text{ \AA}$.^{2,3} In the present case, the magnetic order remains commensurate. Beyond this difference, both substitutions indicate that a certain type of disorder in the charge reservoirs can lead to the cohabitation of two distinct electronic states in CuO_2 planes.

Finally, considering the high ordering temperature, the low value of the staggered moment, and the fact that the intensity decreases at large Q much more rapidly than does the Cu-spin form factor [Fig. 1(c)], we believe that the AF ordering in our Co-substituted sample is analogous to that recently reported in underdoped $\text{YBa}_2\text{Cu}_3\text{O}_{6+x}$ (x

$\sim 0.5-0.6$).^{4,5} There is nevertheless one striking difference: the additional enhancement of the AF intensity observed below T_c is not seen in the present case. The anomalously fast decrease of the magnetic form factor in the well underdoped “pseudogap phase” $\text{YBa}_2\text{Cu}_3\text{O}_{6.6}$,⁵ was interpreted as evidencing a d -wave density-wave order.³¹ Our finding of a similar unusual structure factor in a Co-substituted sample with an optimum T_c where pseudogap behavior is absent, questions this conclusion. The precise reason for the observed structure factor remains unclear at present.

As a conclusion, we observe a Cu(2) site commensurate long range AF order ($T_N \sim 330 \text{ K}$, $\mu \sim 0.14 \mu_B$) in the superconducting high- T_c cuprate $\text{YBa}_2(\text{Cu}_{1-y}\text{Co}_y)_3\text{O}_{7+\delta}$ ($y = 0.013$, $T_c = 93 \text{ K}$). The disorder introduced by substituting magnetic Co atoms in the chains thus leads to the simultaneous presence of superconducting and magnetic order parameters without any strong detrimental interference. The cohabitation of AF and SC can be described as an inhomogeneous state associated with the formation of a “granular” AF phase within a d -wave superconductor.

We wish to thank Pierre Gautier-Picard and Philippe Mendels for fruitful discussions.

¹Y.S. Lee *et al.*, Phys. Rev. B **60**, 3643 (1999).

²J.M. Tranquada *et al.*, Phys. Rev. B **59**, 14 712 (1999).

³N. Ichikawa *et al.*, Phys. Rev. Lett. **85**, 1738 (2000).

⁴Y. Sidis *et al.*, Phys. Rev. Lett. **86**, 4100 (2001).

⁵H.A. Mook *et al.*, Phys. Rev. B **64**, 012502 (2001).

⁶M. Braden *et al.*, Phys. Rev. Lett. **88**, 197002 (2002).

⁷N.D. Mathur *et al.*, Nature (London) **394**, 39 (1998).

⁸A. Amato, Rev. Mod. Phys. **69**, 1119 (1997).

⁹H. Kohno *et al.*, J. Phys. Soc. Jpn. **68**, 1500 (1999).

¹⁰Y. Ohashi *et al.*, Phys. Rev. B **60**, 15 388 (1999).

¹¹J.M. Tarascon *et al.*, Phys. Rev. B **37**, 7458 (1988).

¹²R.S. Howland *et al.*, Phys. Rev. B **39**, 9017 (1989).

¹³F. Bridges *et al.*, Phys. Rev. B **39**, 11 603 (1989).

¹⁴H. Renevier *et al.*, Physica C **220**, 143 (1994); **230**, 31 (1994).

¹⁵W.W. Schmahl *et al.*, Philos. Mag. Lett. **60**, 241 (1989).

¹⁶R. Dupree *et al.*, Physica C **193**, 81 (1992).

¹⁷J. Clayhold *et al.*, Phys. Rev. B **39**, 777 (1989).

¹⁸J.W. Loram *et al.*, Supercond. Sci. Technol. **4**, S184 (1991).

¹⁹M. Matsumura *et al.*, J. Phys. Soc. Jpn. **63**, 2382 (1994).

²⁰C. Vaast *et al.*, Phys. Rev. B **56**, 7886 (1995).

²¹I. Mirebeau *et al.*, Phys. Rev. B **50**, 3230 (1994).

²²H. Casalta *et al.*, Phys. Rev. B **50**, 9688 (1994); E. Brecht *et al.*, *ibid.* **52**, 9601 (1995).

²³P. Zolliker *et al.*, Phys. Rev. B **38**, 6575 (1988).

²⁴C. Bellouard *et al.*, J. Magn. Magn. Mater. **104-107**, 517 (1992).

²⁵J. Rossat-Mignod *et al.*, Physica C, **185-189**, 86 (1991).

²⁶P. Bourges *et al.*, Phys. Rev. B **53**, 876 (1996).

²⁷H.F. Fong *et al.*, Phys. Rev. B **61**, 14 773 (2000).

²⁸Y. Sidis *et al.*, Phys. Rev. Lett. **84**, 5900 (2000).

²⁹H.F. Fong *et al.*, Nature (London) **398**, 588 (2002).

³⁰K.M. Lang *et al.*, Nature (London) **415**, 412 (2002).

³¹S. Chakravarty *et al.*, Phys. Rev. B **63**, 094503 (2001).